

PLASMA ACCELERATOR WITH CLOSED ELECTRON DRIFT AND EXTENDED ACCELERATION ZONE

A. I. Morozov, Yu. V. Esinchuk,
G. N. Tilinin, A. V. Trofimov,
Yu. A. Sharov, and G. Ya. Shchepkin

Translated from Zhurnal Tekhnicheskoi Fiziki, Vol. 42, No. 1,
pp. 54-63, January, 1972
Original article submitted March 29, 1971

INTRODUCTION

Accelerators with "closed" electron drift and extended acceleration zone (ACED) [1-4] are the simplest and most promising of the stationary electromagnetic plasma accelerators; in these accelerators ions are accelerated by the electric field that develops in the plasma. The present work initiates a series of experimental and theoretical investigations of the "single-lens" variant of ACED.¹ The experiments were performed with N₂, Ar, Kr, Xe as working gases at voltages U_d up to 1000 V and discharge currents I_d ≈ 15 A. A schematic diagram of the accelerator is shown in Fig. 1; the dimensions of one model are also indicated.

1. BASIC CHARACTERISTICS OF ACED

An almost radial magnetic field is produced in the annular accelerator channel with dielectric walls; this field satisfies the condition

$$R_L > L_c \gg R_{eL}, \tag{1}$$

where R_{ii} and R_{eL} are the ion and electron Larmor radii, respectively, and L_c is the length of the channel.

The potential difference necessary to produce the longitudinal electric field U_d is applied between the anode and the compensator cathode. The com-

¹The two-lens variant of ACED has been described in [5, 6].

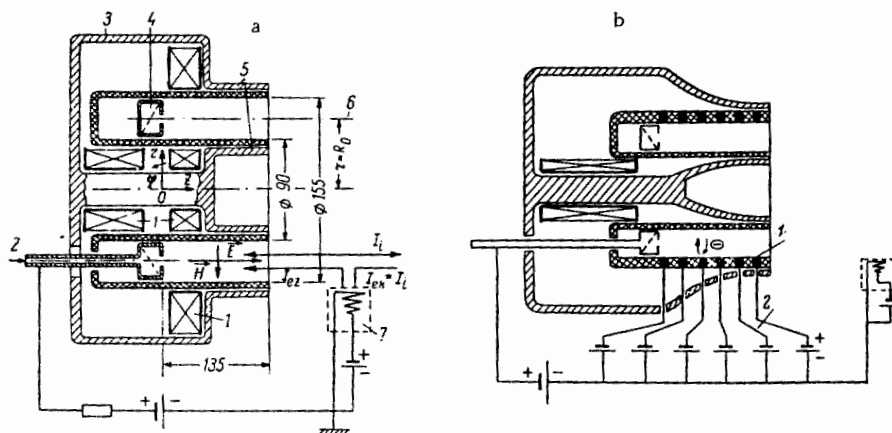


Fig. 1. Basic arrangement of the accelerator. a: 1) Magnetization coils; 2) gas feed; 3) insulators; 4) anode; 5) magnetic circuit with poles; 6) main cylindrical surface; 7) compensator-cathode; b: 1) annular emitting electrodes; 2) power supply.

pensator cathode is the electron source and is placed near the slit of the instrument. Usually it is a gas-discharge element with thermionic cathode and supplies electrons necessary for the ionization of the gas, the compensation of the ion flux from the accelerator, and the compensation of the electron loss at the walls of the channel. This compensation is not always obtained under laboratory conditions.

The discharge takes place in crossed (E⊥H) fields; the gas is fed from outside through the toroidal hollow box-anode with holes for uniform flow of the gas into the channel. When condition (1) is satisfied the electrons execute E⊥H drift along the azimuth, diffusing to the anode. The neutrals arriving from the anode are ionized in this rotating electron cloud.

The ion acceleration occurs without disturbing the quasineutrality since the ion space charge is compensated by the magnetized electrons. When (1) is satisfied the ions leave the channel with an energy (first approximation)

$$\frac{Mv^2}{2} = e\Phi^*, \quad (2)$$

where Φ^* is the potential at the point of formation of the ion. The extended ionization zone and also the presence of oscillations in the system lead to a widening of the energy spectrum of the ions.

In the analysis of the processes in the accelerator, as in most plasma systems, it is necessary to distinguish between the equilibrium configuration and the perturbation. By the equilibrium configuration we mean the stationary flow, in which the distribution of the parameters is similar to that measured experimentally (and averaged over time) and satisfies the stationary conditions of hydrodynamics or kinetics. The main difficulty in the analysis of the equilibrium configuration in the ACED is related to the anomalously large electron mobility in the channel transverse to the magnetic field. Actually, for typical values of the density ($n = 10^{11}$ cm⁻³), the electron temperature ($T_e = 10$ eV), and electric and magnetic fields ($E_z = 30$ V/cm, $H_r = 10^2$ Oe), the longitudinal electron current computed in the Coulomb collision approximation is

$$I_{ez} \approx S_c \frac{\sigma E_z}{(\omega\tau)^2} = 2.5 \cdot 10^{-3} \text{ A} \quad (3)$$

(where $S_c = 10^2$ cm² is the cross section of the channel; $\sigma = 0.9 \cdot 10^{13}$ T^{3/2}). At the same time experiments show (for example, [1]) that I_{ez} is comparable with the longitudinal ion current I_{iz} :

$$I_{ez} \sim (0.3 - 0.5) I_{iz}; \quad |I_d| \equiv |I_{ez} + I_{ez}|, \quad (4)$$

i.e., under the conditions above it is of the order of 1 A. It should be stressed that the high transverse conductivity is important for the operation of ACED; with the Coulomb conductivity alone the entire potential difference U_d is concentrated in a thin sheath at the anode whose thickness is of the order of the electron Larmor radius [7].

The anomalously large transverse electron mobility can be accounted for by two factors.

First there is the conductivity near the wall [8]: Electrons moving freely along the lines of force collide with the wall more often than with ions and neutrals, being reflected from the wall at the Debye discontinuity. For a sufficiently rough surface of the Debye sheath at the insulator the reflection of the electrons can be regarded as a diffusion process. Thus, near the dielectric wall an electron current flows in the direction of the anode; this current is given by

$$I_{ez} = \lambda E = 2\pi c^2 \sqrt{m} \Theta R_{av} \frac{n \sqrt{kT_e}}{H} E, \quad (5)$$

under the assumption that the quantities in (5) have identical values at the inner and outer dielectric walls.² Here, Θ is a dimensionless factor ~ 1 and depends on the extent to which the reflection is a diffusion process; m is the electron mass, $R_{av} = (R_1 + R_2)/2$, and R_1 and R_2 are, respectively, the radii of the inner and outer insulating walls.

An estimate of I_{ez} for the typical conditions considered above yields $I_{ez} \approx 3$ A, which is in agreement with the experimental order of magnitude. A theoretical model of the equilibrium configuration can be constructed in the case of the conductivity in the region adjacent to the wall.

The electrons interact with the external object, i.e., the wall, and therefore the following relations hold in the volume (excluding the ionization zone):

$$0 = \frac{\nabla p_e}{en} + E + \frac{1}{c} [v_e, H], \quad (6a)$$

$$M \frac{dv_i}{dt} = eE + \frac{e}{c} [v_i, H], \quad (6b)$$

in which the electron inertia, the ion temperature, and electron-ion collisions have been disregarded. System (6) must be supplemented by the equation of conductivity (5) of the region near the wall, the continuity equation for both the components with appropriate boundary conditions, and the equation for T_e .

²Otherwise the expression for I_{ez} can be written separately for the inner wall and the outer wall of the channel.

Oscillations in the plasma are the second possible reason for the anomalous electron mobility. In a number of cases it has been shown experimentally [9, 11] that the oscillations play a decisive role in the enhancement of the longitudinal electron current I_{ez} . In the presence of turbulent conductivity the expression for I_{ez} is different from (5) because in this case the conductivity is not determined by local averaging of the flow characteristics. Furthermore, it is necessary to take account of the electron-ion interaction explicitly. Formally the turbulent conductivity can be treated as a certain force K appearing in the equation of motion of the electron component:

$$m \frac{dv_e}{dt} = -eE - \frac{e}{c} [v_e, H] + K + \frac{ej}{c} + \frac{\nabla p_e}{en}. \quad (7a)$$

Obviously it can be assumed that $K \cdot H = 0$. In the ion equation of motion the term $-K$ must be included because the diffusion of electrons is due to the interaction between the electron and ion components

$$M \frac{dv_i}{dt} = eE + \frac{e}{c} [v_i, H] - K \frac{ej}{c} + \frac{\nabla p_i}{en}. \quad (7b)$$

The presence of the terms $\pm K$ in the equations of motion leads to the appearance of the corresponding term in the energy equation for each component, i.e., the anomalous conductivity necessarily leads to anomalous "heating" of ions and electrons.

An analytic expression for K is not available. Its form can only be predicted on the basis of experimental data and present (highly restricted) theories for turbulent processes. Thus a correct model of equilibrium configuration in the regime of zero conductivity cannot yet be constructed. For this reason the model of conductivity in the region adjacent to the wall will be used in the theoretical analysis. The further analysis of the processes in ACED requires a simple form of Eq. (6a). Taking the scalar product of (6a) with H we have

$$-\frac{\partial \Phi}{\partial l} = \frac{1}{en} \frac{\partial p_e}{\partial l}. \quad (8)$$

Here, Φ is the plasma potential and $\partial/\partial l$ denotes differentiation along the lines of force, on which the electron temperature can be assumed constant:

$$T_e = T_e(\gamma), \quad (9)$$

γ is the index designating a line of force. Since the electron pressure $p_e = nkT_e(\gamma)$ we can integrate (8) and obtain an important equation:

$$\Phi - \frac{kT_e(\gamma)}{e} \ln \frac{n}{n_0(\gamma)} = \Phi_T(\gamma). \quad (10)$$

The quantity $\Phi_T(\gamma)$, which is conserved along a line of force, is called the "thermal potential." If T_e is negligibly small, then

$$\Phi \approx \Phi_T(\gamma), \quad (11)$$

which means that the lines of force are equipotentials. It should be noted that (8) is valid even in the case of turbulent conductivity by virtue of the assumption made earlier that $K \cdot H = 0$. Thus at small values of T_e it is possible to produce arbitrary configurations of electric equipotentials in the plasma volume, which can be used for the acceleration and focusing of the ion streams [10]. A given relationship $\Phi_T(\gamma)$ can be obtained either by virtue of the internal conductivity of the channel or through the use of special electrode holders that extend out to the dielectric walls (Fig. 1b). The ACED is a system with a complete set of plasma parameters n, v_i, v_e, p, E, H . The study of the dynamics of compensated ion beams in ACED and their stability will contribute to the development of plasma dynamics as a physical discipline. Also, mastery of the principles of producing electric fields of required configurations in the plasma will facilitate the development of high-current accelerators, plasma-optical systems, and thermonuclear devices. The interest in the theoretical and experimental investigations of the physical processes in the ACED is motivated by these factors. As already mentioned, there is a considerable amount of published work on single-lens ACED, in which the volt-ampere characteristics of the discharge have been determined, the distributions of the potential and the ion current in the channel have been measured, and information about the oscillations in the system has been gathered. Theoretical studies have attempted to develop a model of the ionization instability. In view of the fact that the investigations have been carried out by different groups and deal

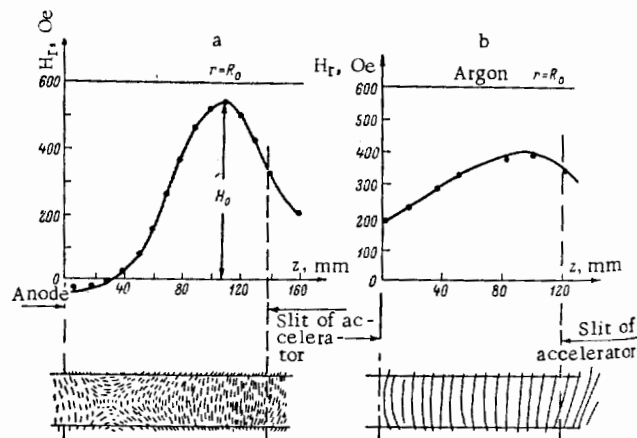


Fig. 2. Distribution of magnetic field in the accelerator channel.

with separate problems, as yet there is no unified picture of the processes in ACED. The effect of the magnetic field structure, the turbulent oscillations, the problem of interaction between the ion stream and the walls, etc., have not been investigated.

In the theoretical and experimental work, conducted at the V. I. Kurchatov Institute of Atomic Energy since 1963, attention has been devoted mainly to a systematic understanding of the factors that determine the pattern of the processes in single-lens ACED and to a search for means to control these processes.

2. MAGNETIC FIELD IN THE CHANNEL

The magnetic system of the accelerator model (Fig. 1) contains three magnetization coils; these make it possible to vary the configuration and the strength of the magnetic field over a wide range. In the present work, however, only those configurations are considered in which the magnetic field H_r increases with the longitudinal coordinate z and $H_z = 0$ for $r = R_{av}$. These configurations are called positive-gradient fields (normal):

$$\nabla_r H \equiv \frac{\partial H}{\partial z} > 0. \quad (12)$$

Two typical magnetic fields are shown in Fig. 2a,b; the variation of the radial component $H_r(z)$ along the channel, measured by a Hall sensor, is also shown for both cases. These relationships correspond to the midpoint of the gap of the ac-

celerator channel $R_{av} = (R_1 + R_2)/2$, where H_z can be assumed to be zero. The configuration of Fig. 2a is characterized by a vanishing magnetic field near the anode. Obviously, by virtue of (10) the curvature of the lines of force facilitates the focusing of the ion stream at the plane $r = R_{av}$. In the case shown in Fig. 2b, the magnetic field near the anode is large and is approximately one half of its maximum value; however, the curvature of the lines of force within the channel is small. In both cases the lines of force are symmetric with respect to the median surface $r = R_{av}$.

3. VOLT-AMPERE CHARACTERISTICS OF THE DISCHARGE

The model of the accelerator is placed in a vacuum chamber having a volume of $\sim 1 \text{ m}^3$, which is evacuated by oil pumps. Under operating conditions (with gas feed \dot{m}) the pressure in the chamber is less than $2 \cdot 10^{-4} \text{ mm Hg}$.

The volt-ampere characteristics of the discharge for different feed rates of the working gas and a fixed magnetic field are shown in Fig. 3a,b. Here, I_m^* denotes the so-called "consumption current"

$$I_m^* = \frac{em}{M} = I_{H^*}.$$

The volt-ampere characteristics can be divided into two segments:

$$\left. \begin{array}{l} 1) I_d \leq I_m^* \\ 2) I_d > I_m^* \end{array} \right\} \quad (13)$$

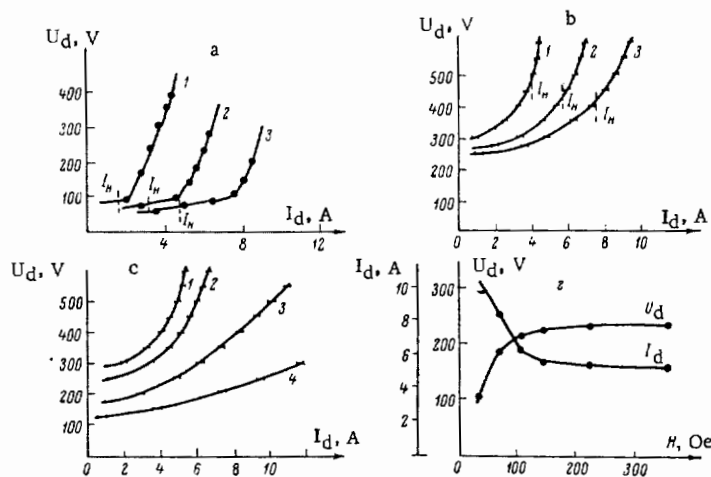


Fig. 3. Volt-ampere characteristics of the discharge in the accelerator. a: Xe, 1) $\dot{m} = 2$; 2) 4; 3) 6 mg/sec, $H_0 = 300$ Oe (Fig. 2b); b: Ar, $I_H = em/M$. 1) $\dot{m} = 1.6 \cdot 10^{-3}$; 2) $2.3 \cdot 10^{-3}$; 3) $3.1 \cdot 10^{-3}$ g/sec, $H_0 = 530$ Oe (Fig. 2a); c: Ar, $\dot{m} = 2 \cdot 10^{-3}$ g/sec. 1) $H_0 = 230$; 2) 265; 3) 133; 4) 67 Oe (Fig. 2a); d: Xe, H) Fig. 2b.

In the first segment, where the increase in P_d , the power supplied to the discharge, causes an increase of the current, the accelerator operates in the regime of incomplete ionization. In the second segment there is almost no increase in I_d , but the discharge voltage U_d increases sharply, corresponding to a regime with complete ionization. The lower the ionization potential of the working gas, the more clearly defined is the transition from the regime of ionization to that of current saturation. For an easily ionizable working material (for example, Xe) the discharge current in the region of saturation can exceed I_m appreciably, indicating either appreciable electron current or an appreciable fraction of doubly charged ions in the ion stream.

When the geometries of the channel and the anode, the material of the dielectric walls, and the configuration of the magnetic field are specified, the discharge voltage U_d is determined by the gas A and the feed rate \dot{m} , the discharge current I_d , and the magnetic field H_0 :

$$U_d = f(A, \dot{m}, I_d, H_0, \Gamma), \quad (14)$$

where Γ represents the geometric and structural factors indicated above. It follows from Fig. 3a, b that the dependence of U_d on the feed m for a given A , H_0 , and Γ can be approximated by the expression

$$U_d = U_0 - U^* \ln \left(1 - \frac{I_d}{\chi \frac{e \dot{m}}{M}} \right). \quad (15)$$

Here, U_0 , U^* , and χ are constants that depend on A , H_0 , and Γ . The lower the ionization potential of the working gas, the lower the values of U_0 and U^* , and the higher the value of χ . The structure of the coefficient χ will be investigated in a later paper. For the accelerator model with magnetic field shown in Fig. 1 and with argon as the working gas the values of these coefficients are as follows: $U_0 \approx 200$ V, $U^* \approx 450$ V, $B = \chi e \dot{m} / M = 1.25$.

If the magnetic field is varied, keeping \dot{m} , A , and Γ constant, then U_d and I_d undergo variations as shown in Fig. 3c,d. These results indicate that there is a critical magnetic field H_{cr} beyond which the changes of the current and voltage are insignificant, i.e., there is a magnetic saturation effect. It should be noted that the variations of the geometric and structural factors also have a noticeable effect on the nature of the function $U_d(I_d)$.

In order to determine the components of the discharge current $I_d = I_{iz} + I_{ez}$ the total ion current I_{iz} in the flux from the accelerator has been measured by a deep cylindrical collector with negative bias (Fig. 4). In the investigated range of the parameters the secondary electron emission is less than 7%. The results of these measurements, presented in Fig. 4, show that in the better regimes the relative value of the longitudinal electron current is

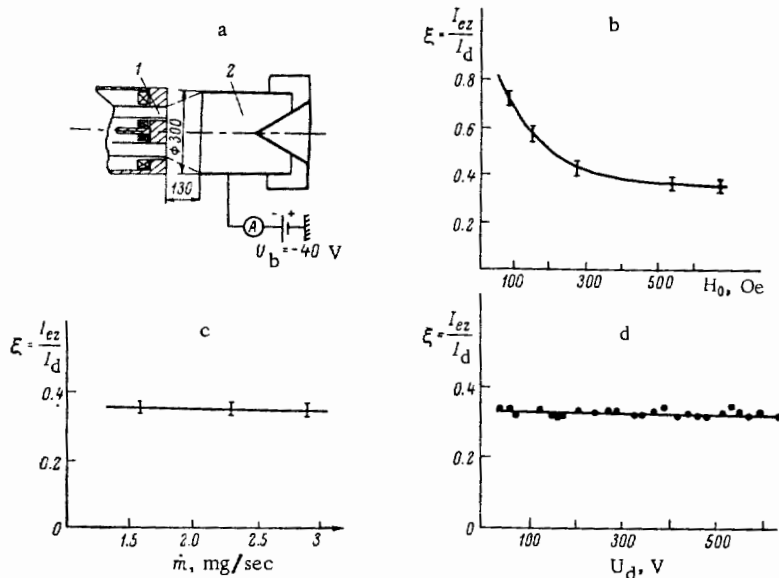


Fig. 4. Ratio of ion and electron currents. a: 1) accelerator, 2) collector; b: $H_0 = 530$ Oe (Fig. 2a), $\dot{m} = 2.3 \cdot 10^{-3}$ g/sec [Ar]; c: Ar, $H_0 = 530$ Oe (Fig. 2a), $U_d = 220$ -600 V; d: $\dot{m} = 2.3 \cdot 10^{-3}$ g/sec [Ar], $H_0 = 530$ Oe (Fig. 2a), $I_{ez}/I_d = 0.35$.

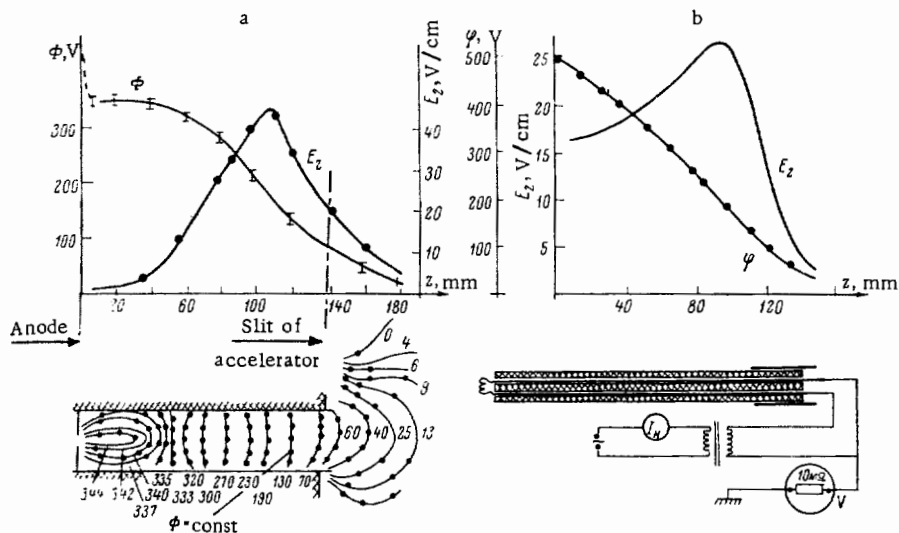


Fig. 5. Measurement of the potential in the accelerator channel by an emitting probe. a) Ar, $\dot{m} = 2.3$ mg/sec, $U_D = 400$ V, $H_0 = 580$ Oe (Fig. 2a); b) Ar, $\dot{m} = 2$ mg/sec, $U_D = 500$ V, $H_0 = 300$ Oe (Fig. 2b).

$$\xi \equiv \frac{I_{ez}}{I_d} \approx 0.35. \quad (16)$$

The variation is small the entire investigated part of the volt-ampere characteristic and is essentially independent of \dot{m} , the feed rate of the working gas. Some increase of ξ is observed in a working gas with a lower ionization potential. Figure 4 shows that the relative value of the electron current ξ is determined by the magnetic field in the channel, or more accurately, by the quantity $\int_{L_H} H_r dz$; the integral is taken over the entire length of the region L_H , where the radial magnetic field exists. In the region of magnetic saturation ($H > H_{cr}$) ξ also remains fixed.

4. DISTRIBUTION OF THE POTENTIAL AND ION CURRENT IN ACCELERATOR CHANNEL

The plasma potential in the accelerator channel is measured by an emitting floating probe; the construction of the probe is shown in Fig. 5. The signal is fed to a cathode voltmeter with input impedance of 10 M Ω . Figure 5 shows the equipotentials of the electric field, $\Phi = \text{const}$, and also the potential distribution $\Phi(z)$ along the channel in the middle of the gap $r = R_{av}$ for different configurations of the magnetic field. A characteristic feature is that the longitudinal electric field E_z develops in the entire accelerator or in a greater

part of it. Where the magnetic field is close to zero the electric field E_z is also small. The longitudinal field E_z is proportional to the local magnetic field since

$$E \sim H^\alpha \quad (\alpha \sim 1). \quad (17)$$

This relationship holds even in the region of magnetic saturation, where the discharge voltage is essentially independent of H . As yet it has not been possible to find the right explanation for the presence of the potential jump near the anode; the magnitude of this discontinuity decreases with increasing U_D and tends to zero in the region of current saturation.

The ion current density is determined with a double electric probe (Fig. 6) with negative bias of the ion collector. The results of the measurements are presented in Fig. 6. The variation of the total ion current I_{iz} along the channel, determined by integrating the current density over the cross section,

$$I_{iz} = \int_{R_1}^{R_2} 2\pi r j_{iz} dr,$$

is also shown in the same figure.

It is evident that in the region near the anode the stream is well formed and does not interact with the channel walls. The ionization of the gas fed into the channel occurs in this region; the ion current increases from a certain value, causing the

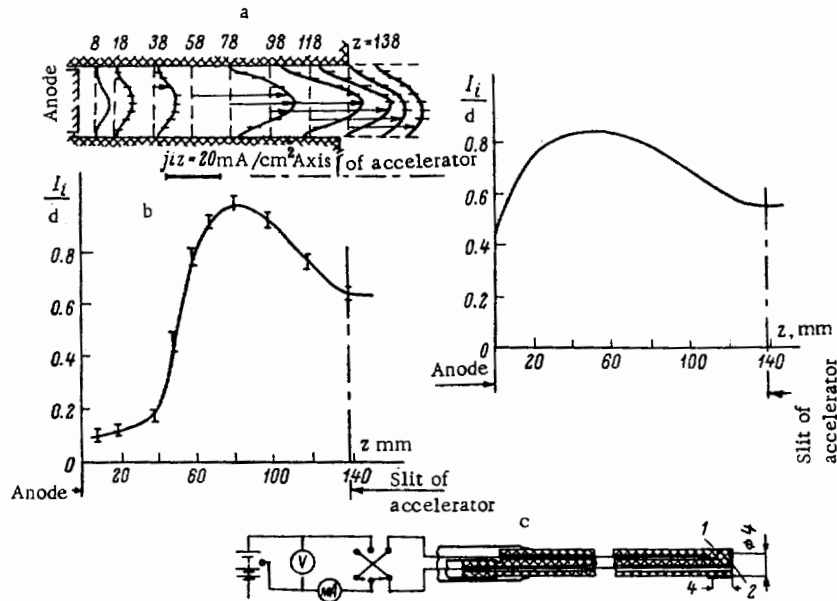


Fig. 6. Distribution of the ion current inside the channel. a: Ar, $\dot{m} = 2.3$ mg/sec, $U_D = 400$ V, $I_D = 5.2$ A, $H = 530$ Oe (Fig. 2a); b: $I_i = 2\pi \int_0^R j_{iz} r dr$; c: 1) ring; 2) collector.

ionization in the immediate vicinity of the anode, to a value comprising $(0.9-0.95)I_D$ at the maximum. An interaction of the beam with the walls, which leads to the loss of ions, is observed in the second half of the channel; as a result the total ion current is reduced to $0.6 I_D$. The ions hitting the walls lose their charge, which must be compensated for by the electrons. This leads to an appreciable increase of the longitudinal electron current passing through the output section of the channel to a value $0.35 I_D$ compared to $(0.05-0.1) I_D$ at the current maximum.

From the known distributions of the potential $\Phi(z)$ and the ion current $I_{iz}(z)$ one can determine the nature of variation of the effective transverse conductivity of the plasma along the channel for the electron component:

$$\sigma_{\perp \text{ eff}} = \frac{j_{ez}}{E} = \frac{I_{ez}}{\pi E (R_2^2 - R_1^2)}. \quad (18)$$

The sharp decrease in the conductivity in the neighborhood of the maximum of the magnetic field (Fig. 7) is noteworthy.

5. DISCUSSION OF THE RESULTS

The experimental results presented above show that the distributions of the potential and the ion current in the channel are very complex. There-

fore it is not possible to obtain a complete analytical expression for the volt-ampere characteristic and to analyze it as a function of the external parameters. Calculations for a number of theoretical models of the ACED will be published later. In this note we restrict ourselves to a quantitative discussion of the results.

First of all it should be noted that in the ideal scheme of ACED with Coulomb conductivity in which the ions do not interact with the walls and are generated in a thin sheath near the anode, the discharge voltage U_D must be independent of H in view of the negligibly small electron current I_{ez} . In this case the discharge current I_D is determined only by the feed rate of the working substance.

The inclusion of an extended (2-3 cm) zone of ionization retaining the Coulomb conductivity must yield values of the discharge voltage U_D which

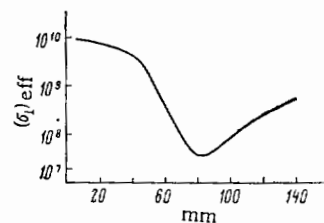


Fig. 7. Transverse conductivity of the plasma in the accelerator channel. $\dot{m} = 2.3$ mg/sec [Ar], $U_D = 400$ V, $I_D = 4$ A, $H_0 = 530$ Oe (Fig. 2a).

would exceed those observed in the experiment by an order of magnitude. The reason for this lies in the fact that under the conditions of strong magnetization of the electrons impeding their diffusion transverse to the magnetic field, a large electron current must flow through the 2-3 cm segment of the channel. The largest discharge voltage would correspond to the regime of incomplete ionization, i.e., the volt-ampere characteristics for an extended zone of ionization and Coulomb conductivity would be "falling" curves. Thus, experimental dependences $U_d(I_d)$ having an opposite nature indicate that in the regime of small ionization the anomalous conductivity of the plasma shows up especially strongly. On the other hand, in the regime with the ionization close to the limiting value the anomalous conductivity gets weakened.

LITERATURE CITED

1. E. C. Lary, R. G. Meyerand, and F. Salz, *Bull. Amer. Phys. Soc., Ser. III*, 7, No. 7, 441 (1962).
2. C. S. Janes and I. Dotson, *Proc. V Symposium on Engng. Aspects of MHD*, MII, 135 (1964); *Transl. Prikladnaya MGD, Moscow* (1965), p. 235.
3. C. O. Brown and E. A. Pinesly, *AIAA J.*, 3, 5, 853 (1965).
4. Chubb and Seikel, *AIAA J.*, 66 (1966).
5. A. I. Morozov, A. Ya. Kislov, and I. P. Zubkov, *ZhETF Pis. Red.*, 7, 224 (1968) [*JETP Lett.*, 7, 172 (1968)].
6. I. P. Zubkov, A. I. Morozov, and A. I. Kislov, *Zh. Tekh. Fiz.*, 40, 2301 (1970) [*Sov. Phys. - Tech. Phys.*, 15, 1796 (1971)].
7. A. V. Zharinov and Yu. S. Popov, *Zh. Tekh. Fiz.*, 37, 294 (1967) [*Sov. Phys. - Tech. Phys.*, 12, 208 (1967)].
8. A. I. Morozov, *PMTF*, No. 3, 19 (1968).
9. G. S. Janes and R. S. Lowder, *Phys. Fluids*, 9, 6, 1115 (1966).
10. A. I. Morozov, *Dokl. Akad. Nauk SSSR*, 163, 1363 (1965) [*Sov. Phys. - Dokl.*, 10, 775 (1966)].
11. E. C. Lary, R. G. Meyerand, and F. Salz, *VI Intern. Conf., Paris, Ses. VC*, July, 1963.